Atmospheric chemistry and aerosols (II)

Dust in the Martian atmosphere

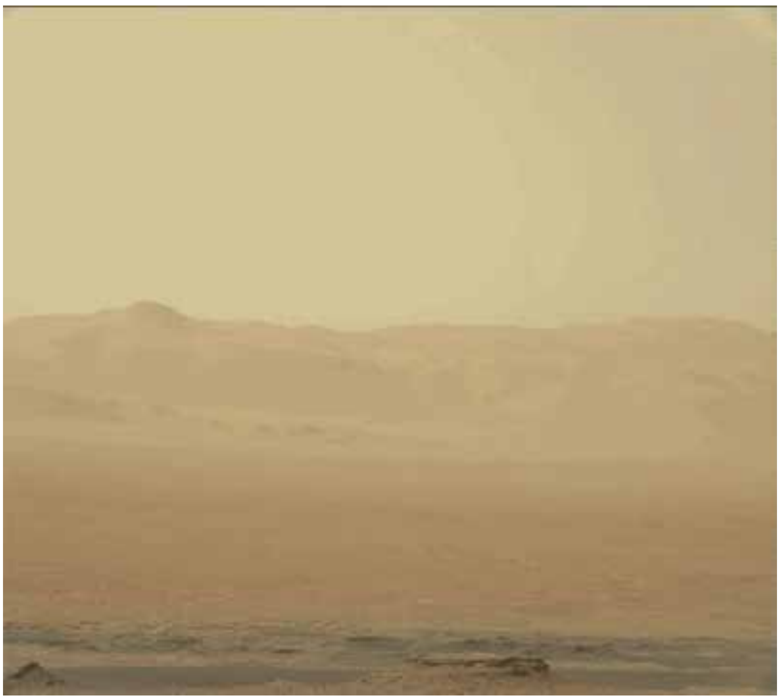

Martian dust storms span the entire planet, in June 2018.
The image was taken from the NASA's rover *Curiosity*

Dust in the Martian atmosphere

- Micrometer-sized small mineral particles float in the atmosphere with a background optical thickness of 0.1-0.5.
- The dust loading changes with time and space.
- The dust serves as a heat source in the atmosphere by absorbing sunlight.

Seasonal variation of optical thickness in infrared
(Smith et al. 2004)

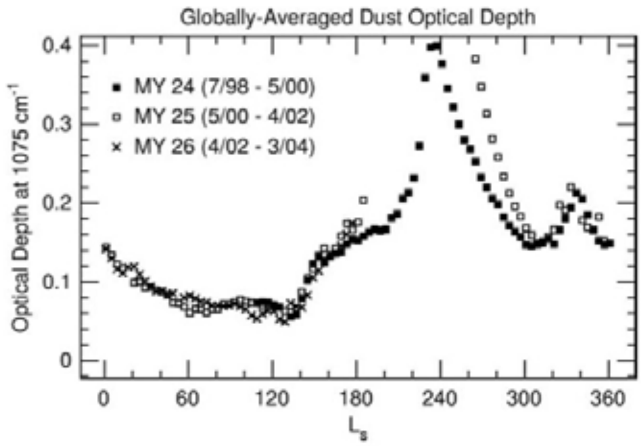

Fig. 7. Globally-averaged daytime (local time ~ 1400) dust optical depth at 1075 cm^{-1} (scaled to an equivalent 6.1-mbar pressure surface) as a function of season (L_S). Three martian years are represented: Mars Year 24 (MY 24) (■), MY 25 (□), MY 26 (×). During the planet-encircling dust storm of 2001 (MY 25), globally-averaged dust opacity reached 1.3 at $L_s = 205$–$215°$.

Seasons of Mars

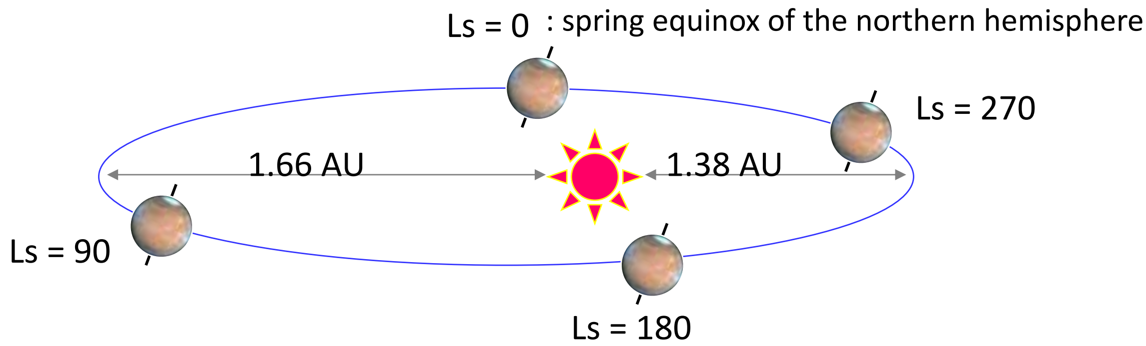

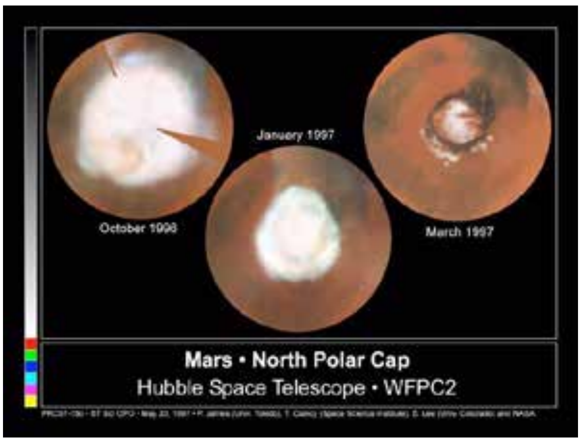

- 火星は公転軌道の離心率が大きいため季節変化が著しく南北非対称
- 南半球の夏に太陽までの距離が近くなる

Dust as a heat source

- Absorption of solar radiation
  - much stronger than the greenhouse effect of CO_2, which is only several kelvins
  - much stronger than cloud albedo effect and latent heat

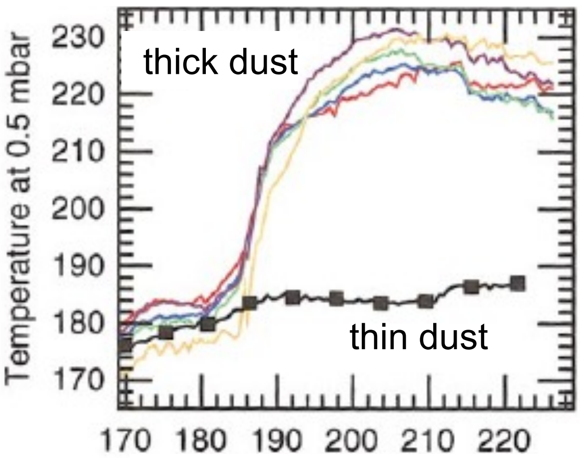

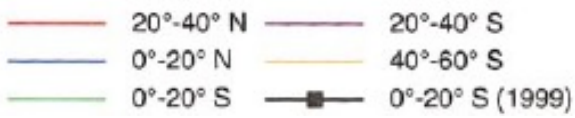

40 K difference between thick-dust year and thin-dust year

Smith et al. (2002)

Radiative-convective model

Gierasch & Goody (1972)

without dust

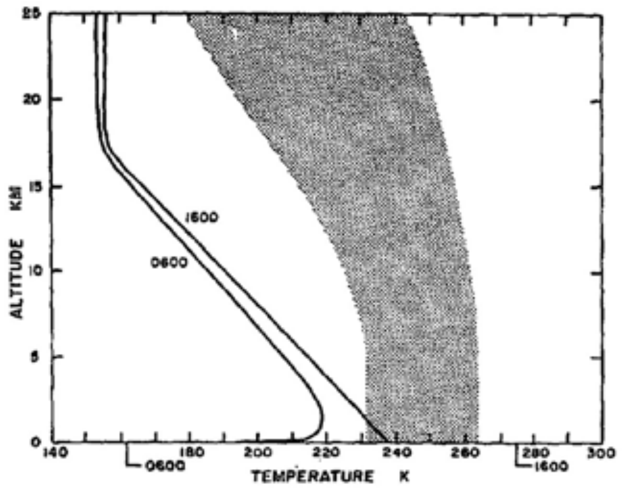

FIG. 1. Martian temperature calculations. The stippled area represents temperatures reported by Kliore *et al.* (1972) and Hanel *et al.* (1972). The lines are theoretical profiles for a pure CO_2 atmosphere, at 1600 and at 0600 hours (the coldest time). Both theory and observation refer to mid-latitude summer conditions. The tags indicate the ground temperatures. In the case of the 1600 theoretical profile a strong boundary layer is indicated.

with dust

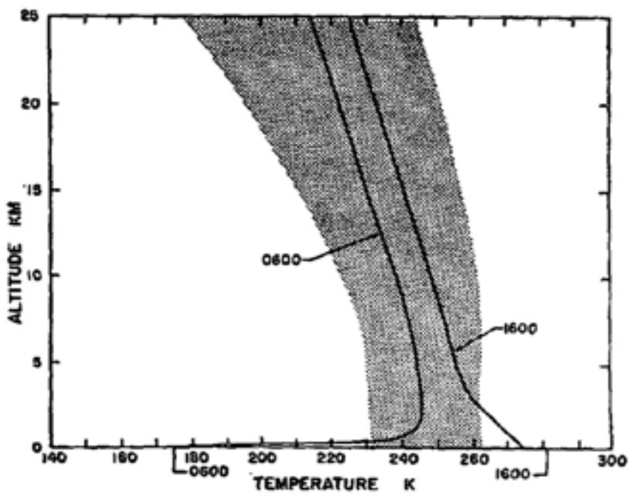

FIG. 2. Same as Fig. 1 except that the atmosphere contains an extra solar absorber, evenly mixed with the atmosphere at all levels, and having an optical depth of 0.10 at all wavelengths. Note the weak boundary layer at 1600.

Dust storms on Mars

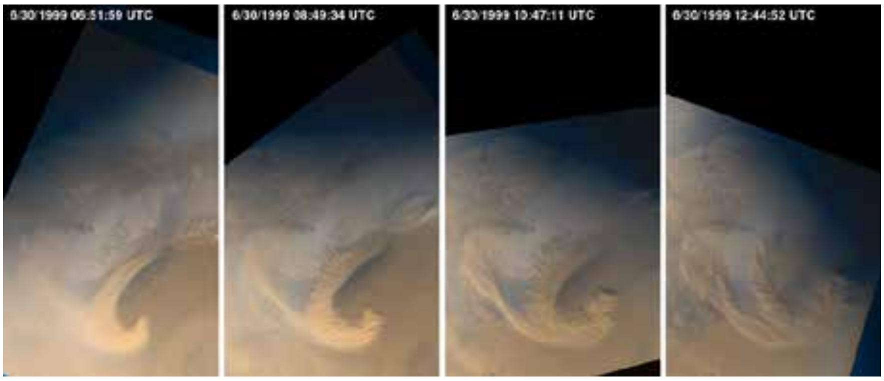

regional storm

Seasonal variation of optical thickness in infrared
(Smith et al. 2004)

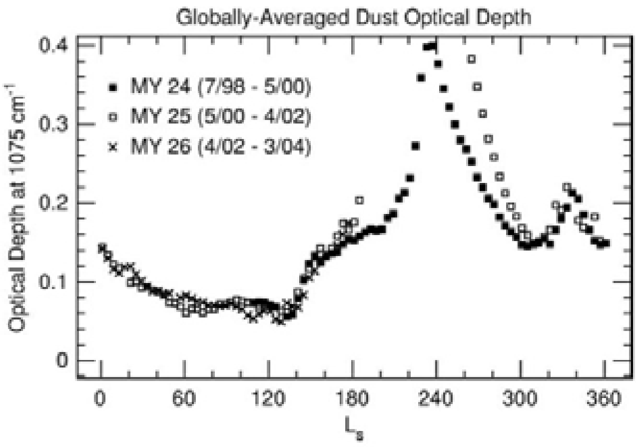

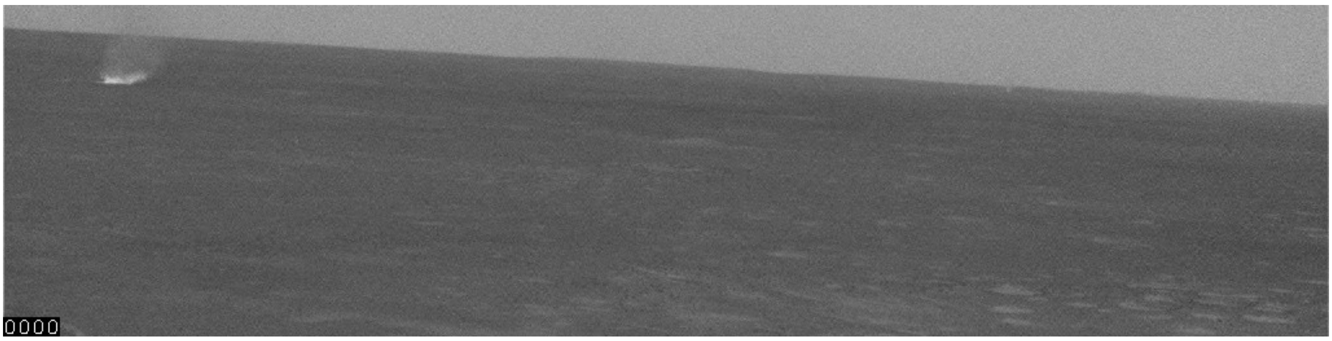

Dust devils

- Source of background atmospheric dust ?

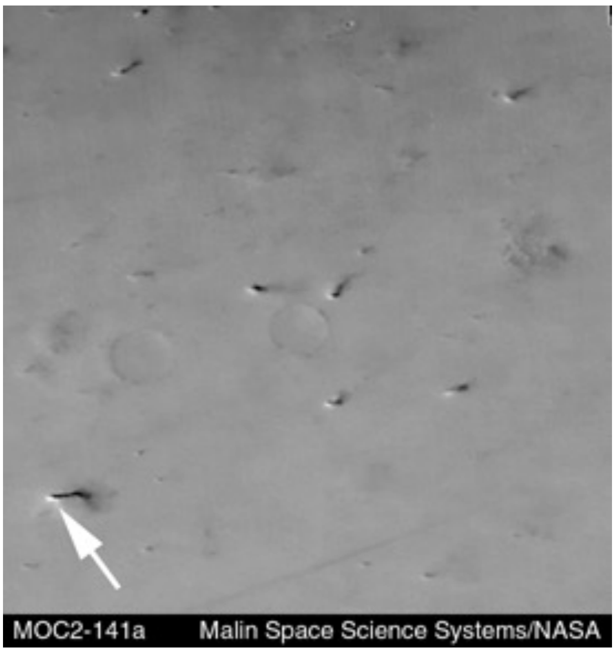

Distribution of atmospheric dust

- Origin of the “background” dust is unknown
- Maximum mixing ratio at 10−20 km altitudes

Smith et al. (2004)

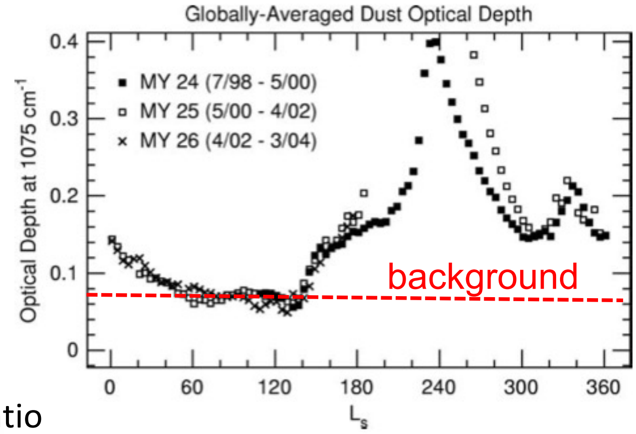

Meridional distribution of dust mixing ratio

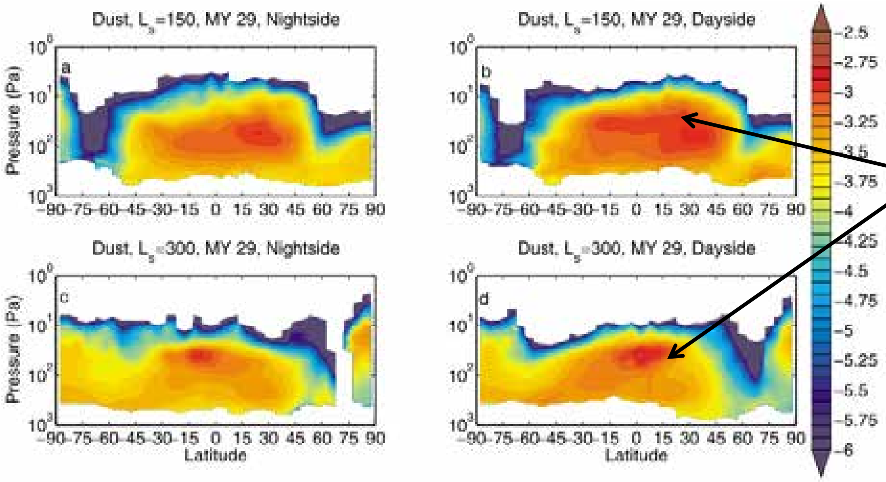

Detached dust layers

Heavens et al. (2011)

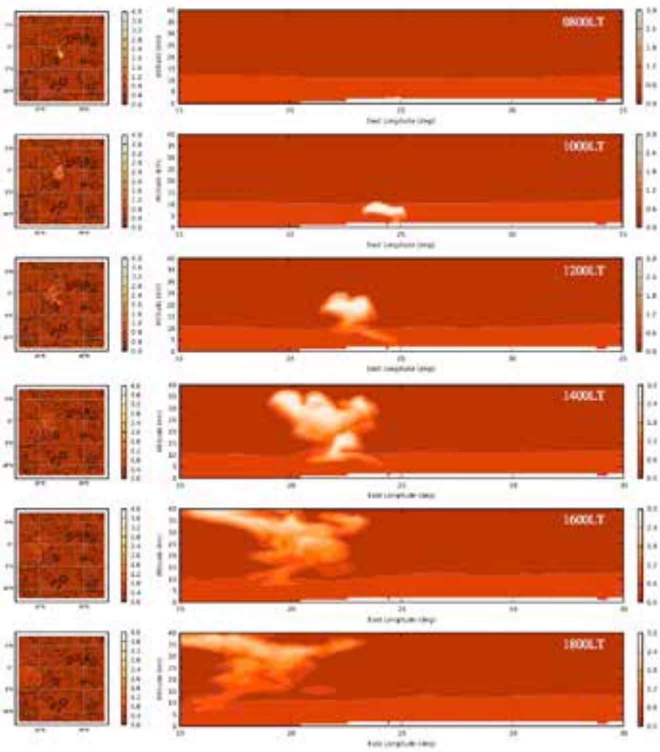

Figure 12. The LMD-MMM storm simulation with lifting and no initial dust perturbation. Same as Figure 4 except that local times range from 0800 to 1800 and longitude-altitude sections are obtained at latitude 1.5°S.

“Rocket dust storm”

Modeling by Spiga et al. (2013)

Dust plumes continuously get buoyancy through solar heating

Global dust storm

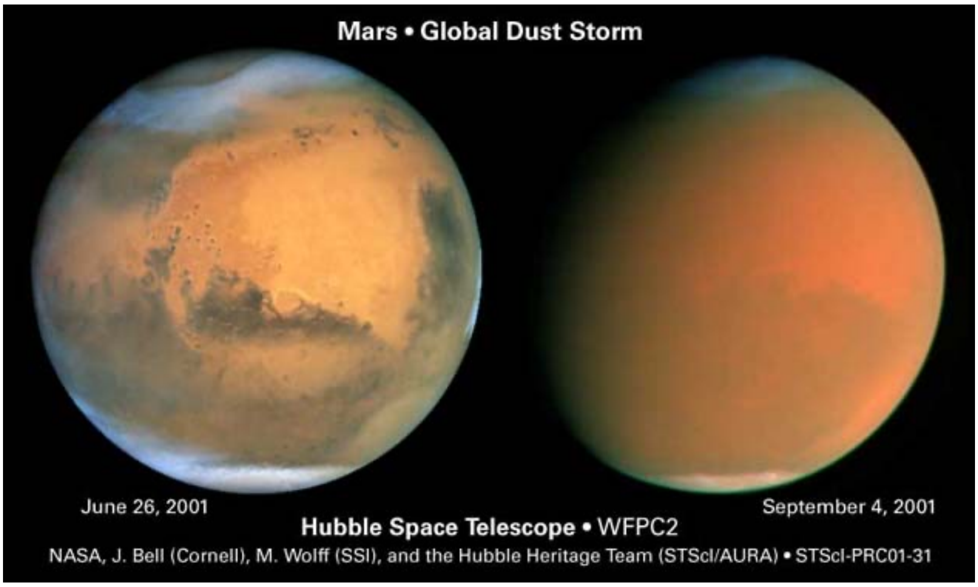

- Global dust storms tend to occur in southern spring-summer
- Positive feedback between dust heating and the intensification of winds is expected in the development of global dust storms.

H_2O ice clouds on Mars

HST Mars image

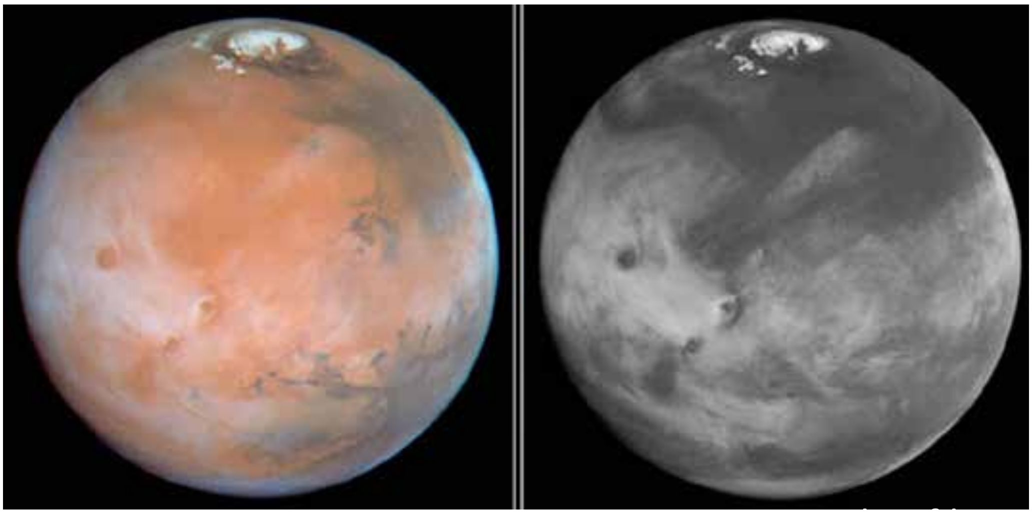

color composite — blue (410 nm)

Seasonal variation of dust, clouds, and H_2O vapor observed by an infrared spectrometer (TES) on Mars Global Surveyor

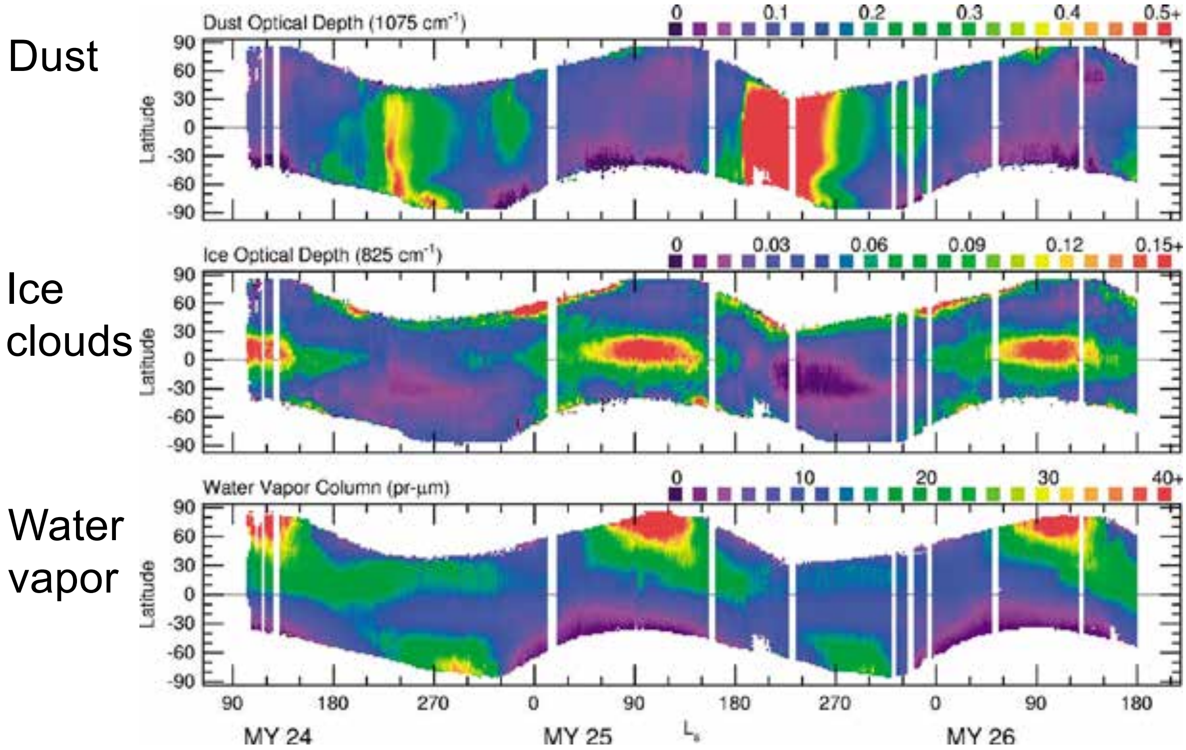

Smith, Icarus 167 (2004) 148–165

Seasonal cycle of Martian water

- 北極冠の消長が全体を駆動
- 北半球の春～夏に北極冠が昇華して北極域の水蒸気濃度が上昇、これが(この時期の弱い)水平渦で低緯度に拡散的に運ばれる。
- 低緯度に運ばれた水蒸気の一部は赤道越えのハドレー循環で南半球へ
- 北半球の秋～冬には北極冠で凝結により水蒸気濃度が低下し、南北濃度勾配が逆転するため、傾圧不安定などに伴う水平渦で低緯度から北極域に水蒸気が拡散的に戻る。低緯度の水蒸気量はそれまでの水蒸気輸送の履歴で決まる。

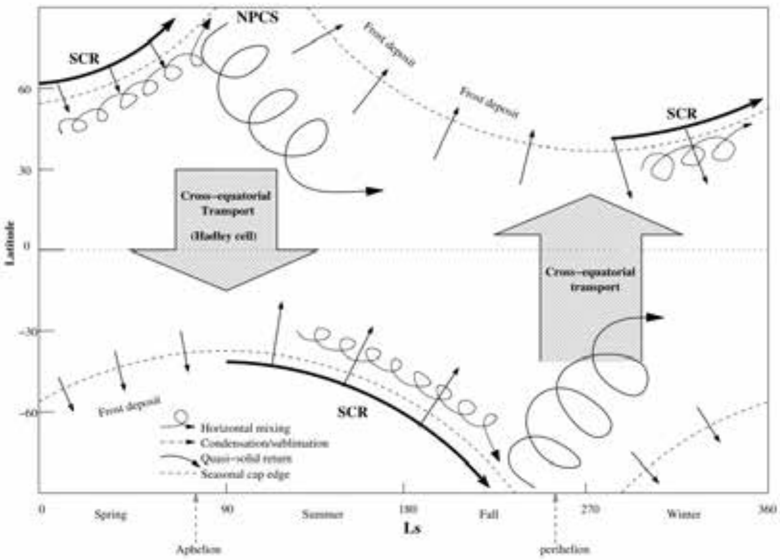

Figure 3. Chart describing the principal events affecting the Martian water cycle over the course of a year. NPCS stands for North Polar Cap Sublimation; SCR stands for Seasonal Cap Recession.

Polar caps: H_2O ice + CO_2 ice

- Seasonal variation
- Residual polar caps in summer
  - H_2O only on the north
  - H_2O + CO_2 on the south ← mystery
- Southern CO_2 ice seems to serve as a cold trap of H_2O

North

South

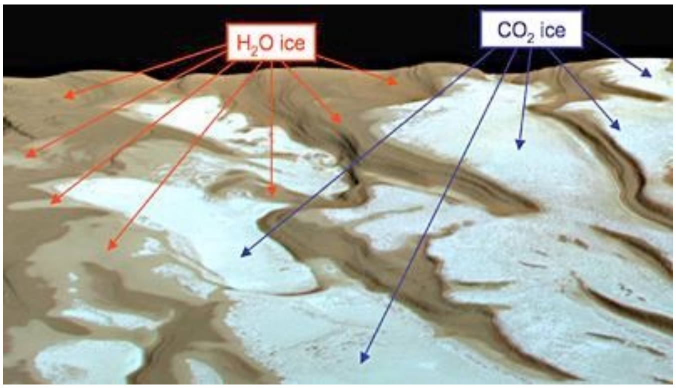

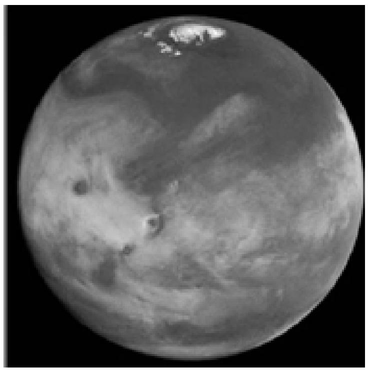

Water transport by Hadley circulation

- Warmer southern summer than northern favors net northward transport of water.

H_2O clouds

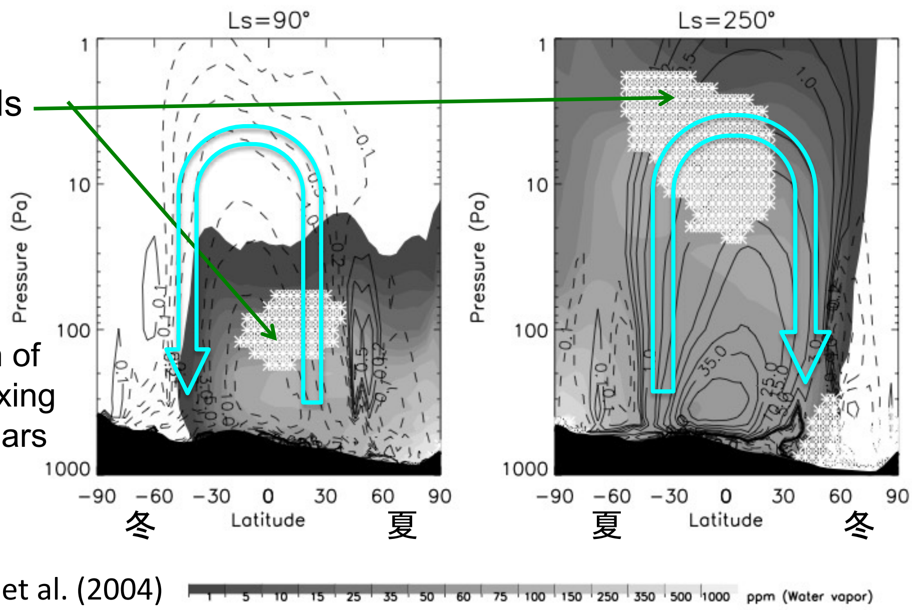

Distribution of H_2O ice mixing ratio in a Mars GCM

Montmessin et al. (2004)

Supersaturation of water vapor on Mars

SPICAM on Mars Express (Maltagliati et al. 2011)

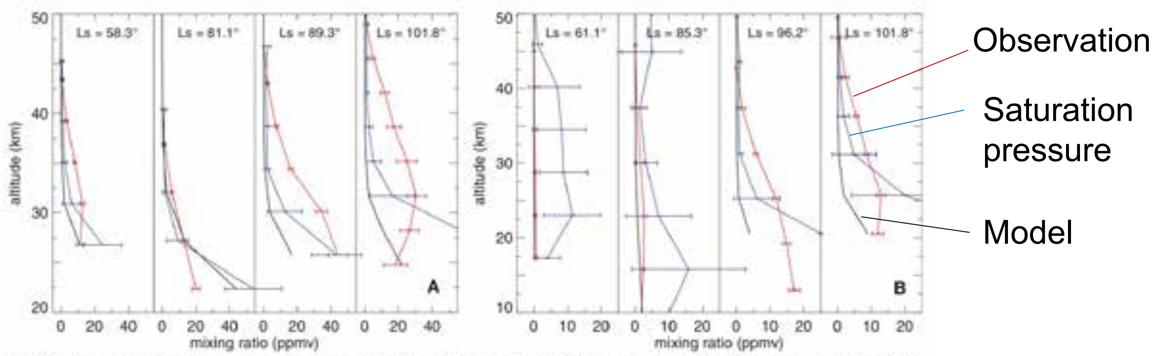

Fig. 2. Selection of typical water vapor volume–mixing ratio profiles in the (**A**) northern and (**B**) southern hemisphere. Black curve, modeled profile by the LMD-GCM; red curve, the retrieved SPICAM results; blue curve, saturation water vapor–mixing ratio. Supersaturation exists where the red values are greater than the blue ones.

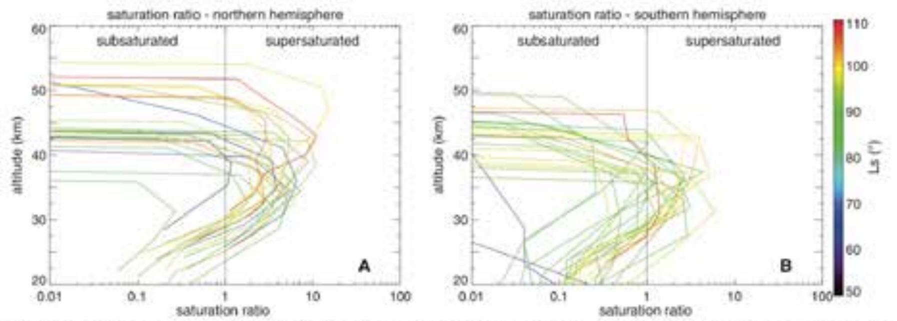

Fig. 3. Saturation ratio for all orbits of the campaign. (**A**) Northern hemisphere. (**B**) Southern hemisphere. The vertical line marks the value of 1, which corresponds to the saturated state.

Vertical distribution of water vapor on Mars during the course of a Mars year

Shaposhnikov et al. (2019)

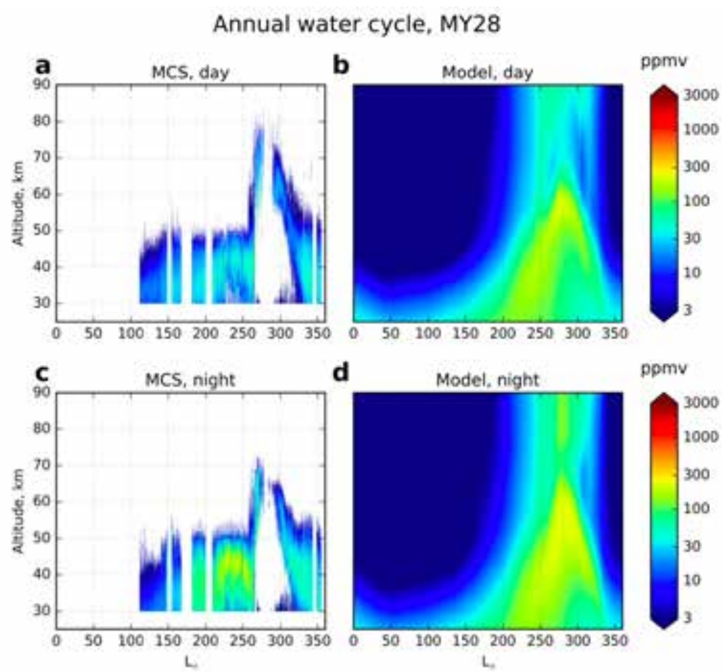

Figure 4. Vertical distribution of the total water (vapor+ice) content derived from the Mars Climate Sounder (MCS) measurements (left column) [*Heavens et al.*, 2018] and simulated with the MPI-MGCM (right column) for the MY28: for the day side (~15:00 local time, upper row) and night side (03:00 local time, lower row). In all panels, the values were averaged over longitudes and latitudes. In the simulations, the averaging over 14:00–16:00 and 02:00–04:00 local times was performed.

Mars Odyssey

Neutron Spectrometer (NS) and
High-Energy Neutron Detector
(HEND)

Subsurface ice

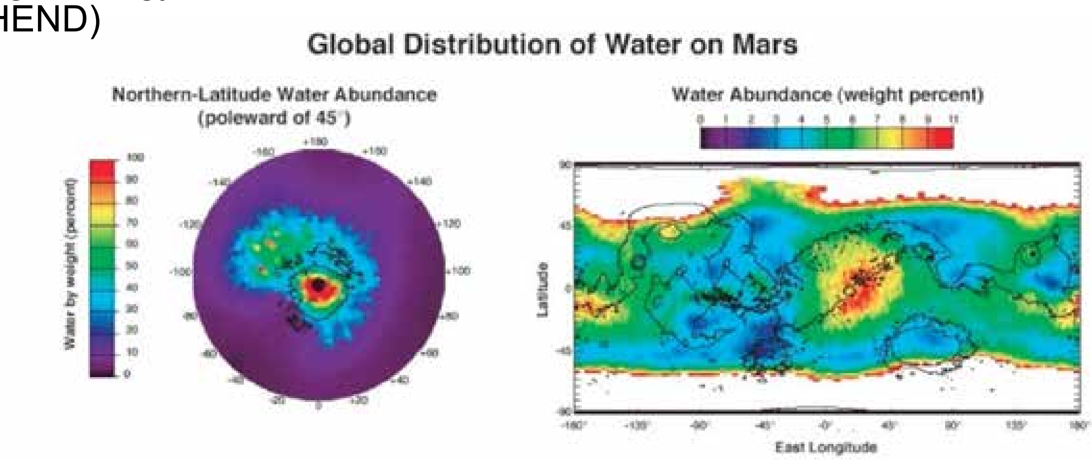

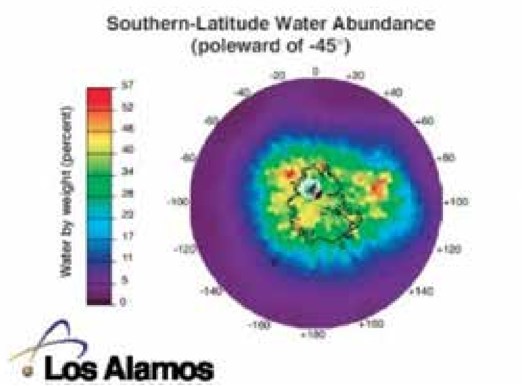

Phoenix Mars Lander

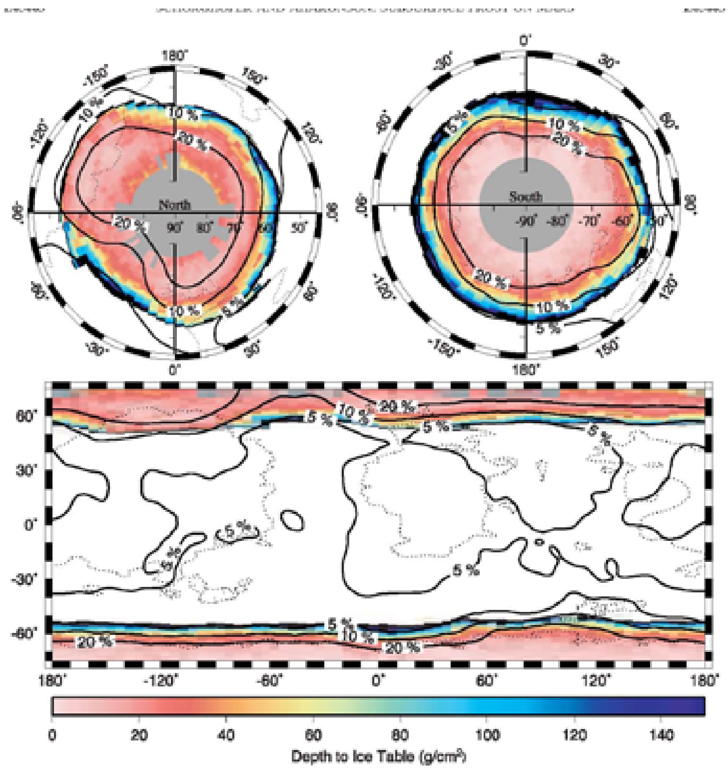

Figure 8. Color indicates depth to the ice table in g cm^{-2} when ice is in equilibrium with the atmospheric water vapor. Ground ice is unstable in the white area. Black segments indicate finite burial depths larger than 150 g cm^{-2}. Missing data points are shown in gray. Assumed volume fraction of ice is 40%, but the geographic boundary between icy and ice-free soil is independent of the ice fraction. Solid contours indicate water-equivalent hydrogen content in percent determined from neutron spectroscopy [*Feldman et al.*, 2004]. The dotted lines are 200 J m^{-2}K^{-1}s$^{-1/2}$ contours of thermal inertia.

Schorghofer and Aharonson (2005)

Comparison with models

Near equilibrium ?

色：　大気中の水蒸気との平衡状態を仮定して計算される氷床までの深さ

実線：　中性子分光観測から見積もられた水含有量

→現在の気候とだいたい平衡状態か

Chemistry of gas giants

Lodders, 2010

Many of the gases observed in their atmospheres are hydrides, which are thermodynamically stable forms in the H_2-rich atmospheres (e.g., CH_4, NH_3, H_2O, H_2S, PH_3, GeH_4, and AsH_3).

These gases (except H_2O and H_2S) are photochemically destroyed by UV sunlight in the stratosphere to produce disequilibrium species (e.g., ethane C_2H_6, acetylene C_2H_2, and ethylene C_2H_4, hydrazine N_2H_4).

The disequilibrium species react with H_2 to reform hydrides once they are transported downward into the hot, high pressure regions.

Table 2. *Composition of the Atmospheres of Jupiter, Saturn, Uranus, and Neptune*

Gas	Jupiter[a]	Saturn	Uranus	Neptune
H_2	86.4 ± 0.3%	88 ± 2%	~82.5 ± 3.3%	~80 ± 3.2 %
^4He	13.6 ± 0.3%	12 ± 2%	15.2 ± 3.3 %	19.0 ± 3.2 %
CH_4	$(1.81 \pm 0.34) \times 10^{-3}$	$(4.7 \pm 0.2) \times 10^{-3}$	~2.3 %	~1-2 %
NH_3	$(6.1 \pm 2.8) \times 10^{-4}$	$(1.6 \pm 1.1) \times 10^{-4}$	<100 ppb	<600 ppb
H_2O	520^{+340}_{-240} ppm	2–20 ppb		
H_2S	67 ± 4 ppm	<0.4 ppm	<0.8 ppm	<3 ppm
HD	45 ± 12 ppm	110 ± 58 ppm	~148 ppm	~192 ppm
$^{13}CH_4$	19 ± 1 ppm	51±2 ppm		
C_2H_6	5.8 ± 1.5 ppm	7.0 ± 1.5 ppm		
PH_3	1.1 ± 0.4 ppm	4.5 ± 1.4 ppm		
CH_3D	0.20 ± 0.04 ppm	0.30 ± 0.02 ppm	~8.3 ppm	~12 ppm
C_2H_2	0.11 ± 0.03 ppm	0.30 ± 0.10 ppm	~10 ppb	60^{+140}_{-40} ppb
HCN	60 ± 10 ppb	<4 ppb	<15 ppb	0.3 ± 0.15 ppb
HC_3N			<0.8 ppb	<0.4 ppb
C_2H_4	7 ± 3 ppb	~0.2 ppb[b]		
CO_2	5-35 ppb	0.3 ppb	40 ± 5 ppt	
C_2H_6			10 ± 1 ppb	$1.5^{+2.5}_{-0.5}$ ppm
CH_3C_2H	2.5^{+2}_{-1} ppb	0.6 ppb	0.25 ± 0.03 ppb	
CO	1.6 ± 0.3 ppb	1.4 ± 0.7 ppb	<40 ppb	0.65 ± 0.35 ppm
CH_3CN				<5 ppb
GeH_4	$0.7^{+0.4}_{-0.2}$ ppb	0.4 ± 0.4 ppb		
C_4H_2	0.3 ± 0.2 ppb	0.09 ppb	0.16 ± 0.02 ppb	
AsH_3	0.22 ± 0.11 ppb	2.1 ± 1.3 ppb		

[a] ^3He 22.6±0.7 ppm, Ne 21±3 ppm, Ar 16±3 ppm, Kr 8±1 ppb, Xe 0.8±0.1 ppb.
[b] assuming a total stratospheric column density of 1.54%10^{25} cm^{-2}.
From Lodders & Fegley 1998 and updates: Mahaffy et al. 2000, Atreya et al. 2003, Lodders 2004, Wong et al. 2004

Cycle of hydrogen-bearing species on giant planets

Catling & Kasting (2017)

$$2CH_4 + \text{photons} \rightarrow \underbrace{C_2H_6 + H_2}_{\text{ethane + hydrogen}}$$

$$2nCH_4 + \text{photons} \rightarrow \underbrace{(C_2H_2)_n + 3nH_2}_{\text{polyacetylene + hydrogen}}$$

$$6nCH_4 + \text{photons} \rightarrow \underbrace{(C_6H_6)_n + 9nH_2}_{\text{polyaromatic hydrocarbons + hydrogen}}$$

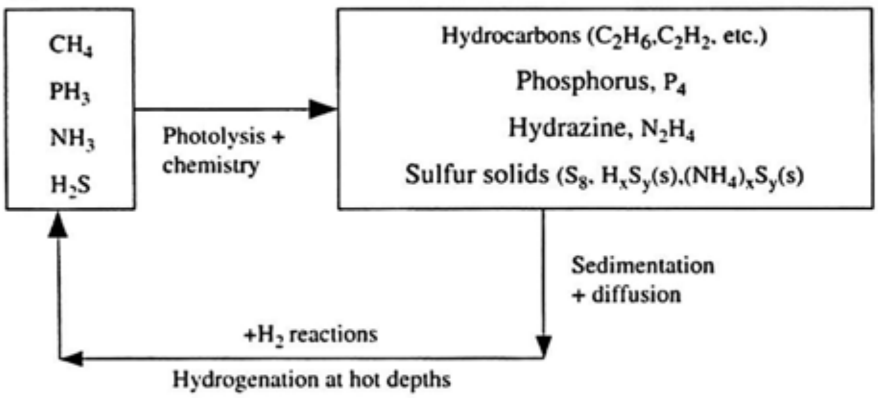

Clouds

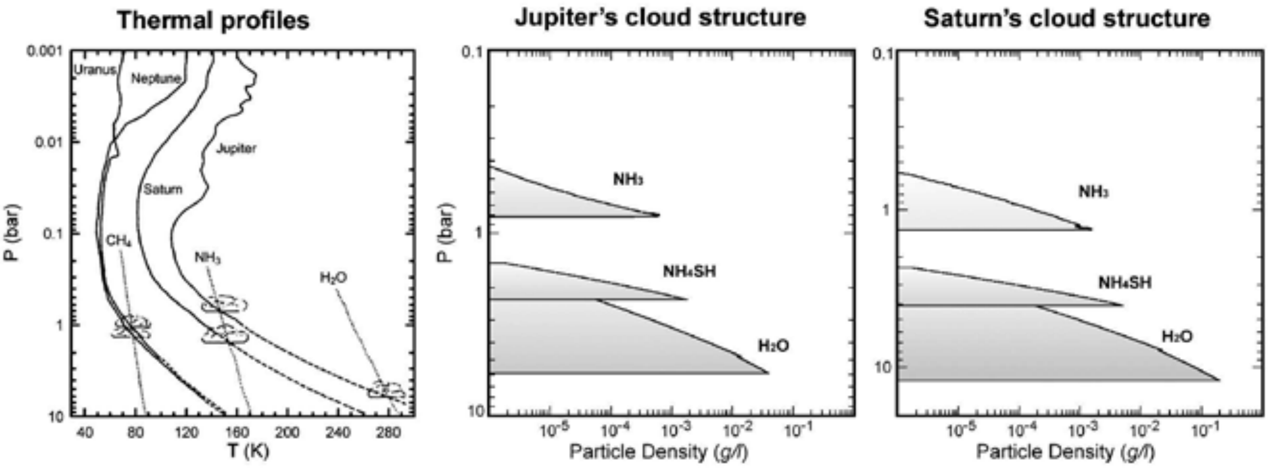

Sanchez-Lavega et al.

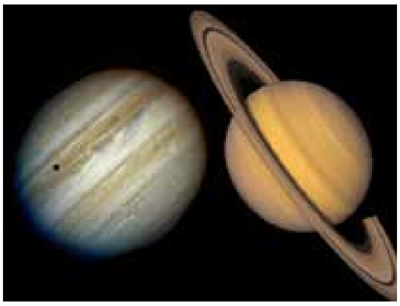

Galileo probe (entry: December 7, 1995)

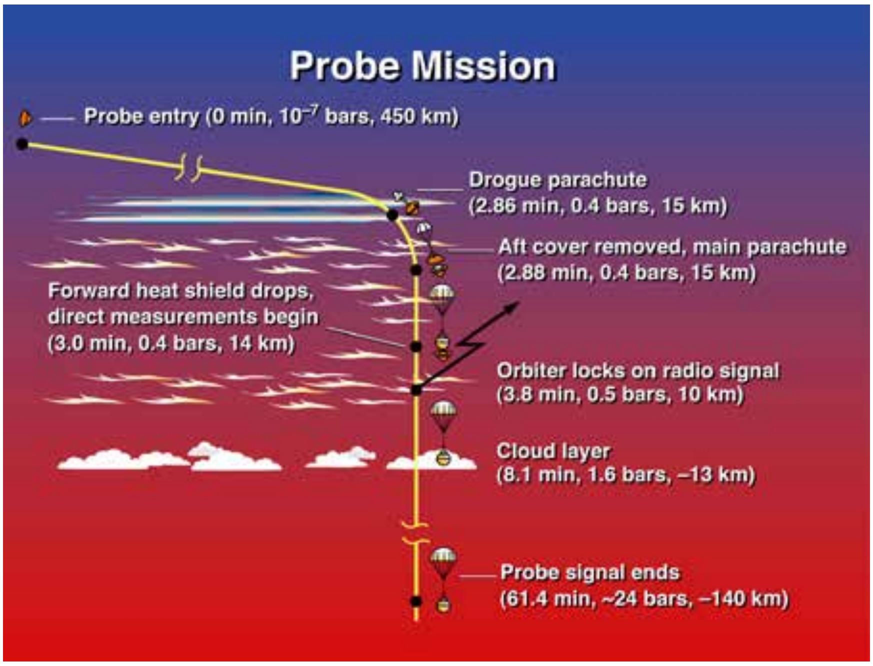

Dry atmosphere ?

- Brightness of the sky abruptly drops off at a pressure level of 0.6 bars, indicating an **ammonia cloud layer** above this height. The tenuous cloud layer detected by the NEP was *not* seen by this experiment.
- **Clouds are patchy and that the Probe went through a relatively clear area**.
- **The atmosphere has much less oxygen than the Sun's atmosphere, implying a surprisingly dry atmosphere.**
- Planetary scientists had expected **oxygen** to be enriched relative to the solar value due to impacts by comets and other small bodies over the 4.5 billion years.

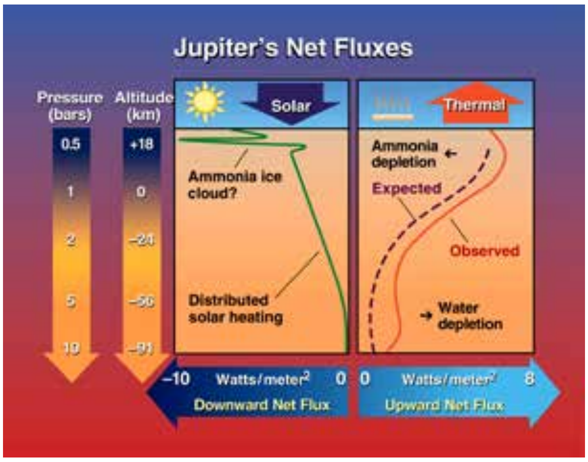

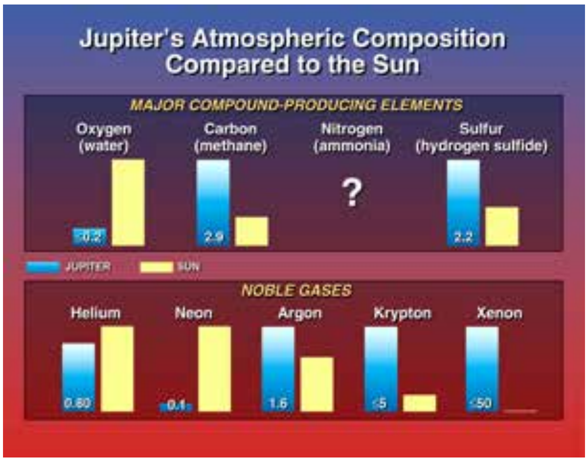

The probe apparently entered a special location

The Probe entry site is near the edge of a so-called infrared "**hot spot**". These "hot spots" are believed to represent regions of diminished clouds on Jupiter.

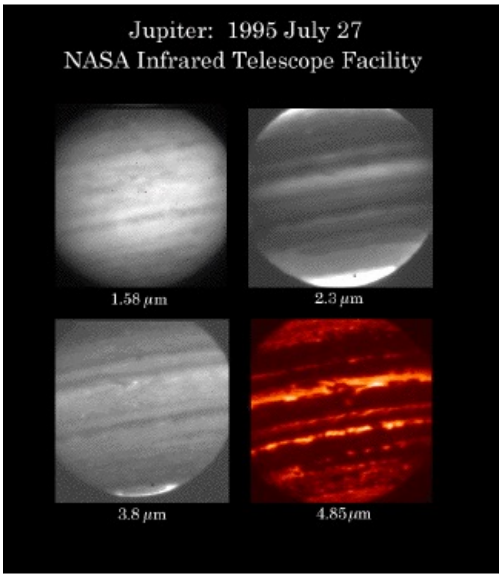

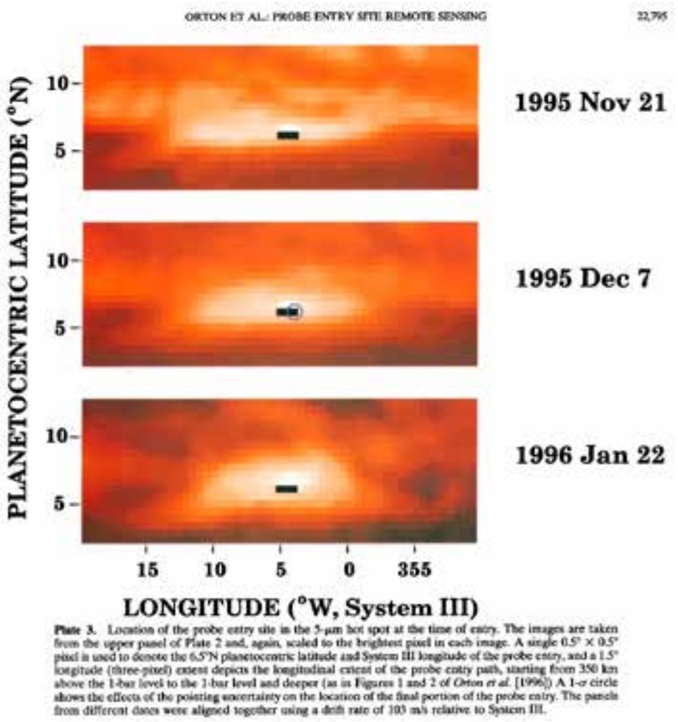

Orton et al. 1998

Atmospheric chemistry on Titan

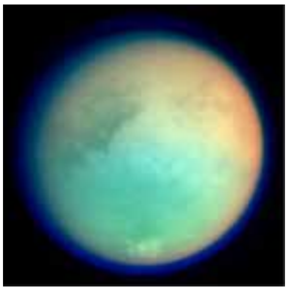

Atmospheric composition of Titan (Coustenis 2007)

Constituent	Mole Fraction (atm. altitude level)
Major	
Molecular nitrogen, N_2	0.98
Methane, CH_4	4.9×10^{-2} (surface)
	$1.4–1.6 \times 10^{-2}$ (stratosphere)
Monodeuterated methane, CH_3D	6×10^{-6} (in CH_3D, in stratosphere.)
Argon, ^{36}Ar	2.8×10^{-7}
^{40}Ar	4.3×10^{-5}
Minor	
Hydrogen, H_2	~0.0011
Ethane, C_2H_6	1.5×10^{-5} (around 130 km)
Propane, C_3H_8	5×10^{-7} (around 125 km)
Acetylene, C_2H_2	4×10^{-6} (around 140 km)
Ethylene, C_2H_4	1.5×10^{-7} (around 130 km)
Methylacetylene, CH_3C_2H	6.5×10^{-9} (around 110 km)[a]
Diacetylene, C_4H_2	1.3×10^{-9} (around 110 km)[a]
Cyanogen, C_2N_2	5.5×10^{-9} (around 120 km)[a]
Hydrogen cyanide, HCN	1.0×10^{-7} (around 120 km)[a]
	5×10^{-7} (around 200 km)[b]
	5×10^{-6} (around 500 km)[b]
Cyanoacetylene, HC_3N	1×10^{-9} (around 120 km)[a]
	1×10^{-7} (around 500 km)[b]
Acetonitrile, CH_3CN	1×10^{-8} (around 200 km)[c]
	1×10^{-7} (around 500 km)
Water, H_2O	8×10^{-9} (at 400 km)[d]
Carbon monoxide, CO	4×10^{-5} (uniform profile)[e]
Carbon dioxide, CO2	1.5×10^{-8} (around 120 km)

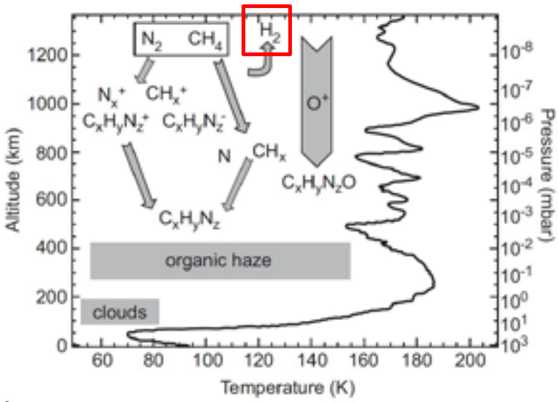

Vuitton et al. (2014)

Figure 7.1 Summary of our current understanding of Titan's atmospheric chemistry, from N_2 and CH_4 to minor gas species, then to macromolecules and organic aerosols. The temperature profile is a smoothed version of the HASI profile (Fulchignoni et al., 2005).

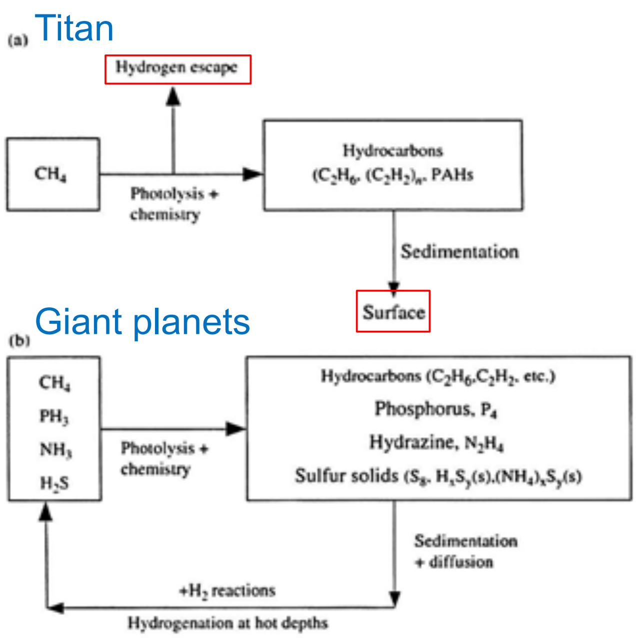

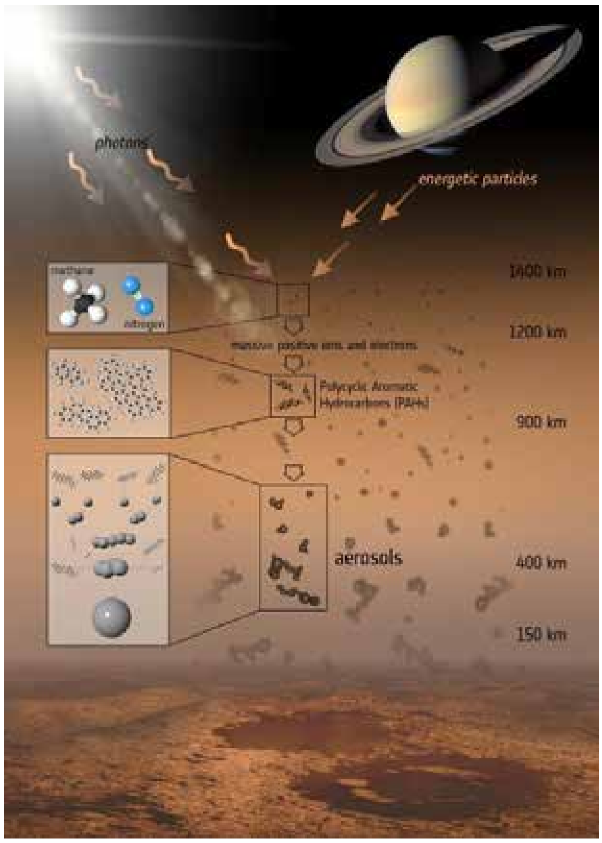

Catling & Kasting (2017)

© NASA

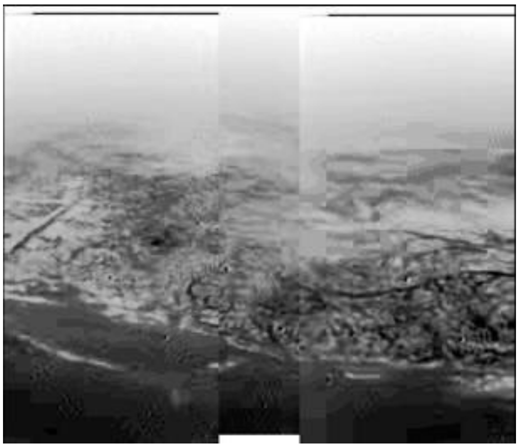

Huygens’ touchdown

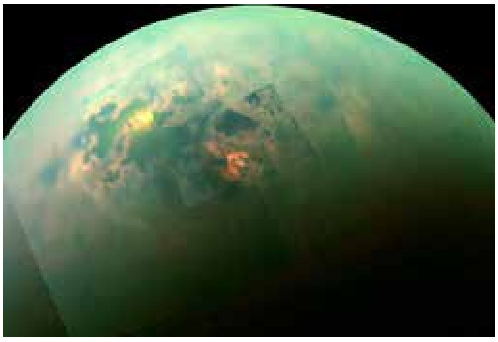

Cassini's Visual and Infrared Mapping Spectrometer (VIMS)